Human-Centered Robotics and Interactive Haptic Simulation

Oussama Khatib, Oliver Brock*, Kyong-Sok Chang,
Diego Ruspini, Luis Sentis, Sriram Viji

Robotics Laboratory, Department of Computer Science
Stanford University, Stanford, California 94305
email: {khatib, kcchang, ruspini, lsentis, sviji}@cs.stanford.edu

*Laboratory for Perceptual Robotics
Department of Computer Science
University of Massachusetts Amherst, Massachusetts 01003
email: oli@cs.umass.edu

Abstract

A new field of robotics is emerging. Robots are today moving towards applications beyond the structured environment of a manufacturing plant. They are making their way into the everyday world that people inhabit. The paper focuses on models, strategies, and algorithms associated with the autonomous behaviors needed for robots to work, assist, and cooperate with humans. In addition to the new capabilities they bring to the physical robot, these models and algorithms and more generally the body of developments in robotics is having a significant impact on the virtual world. Haptic interaction with an accurate dynamic simulation provides unique insights into the real-world behaviors of physical systems. The potential applications of this emerging technology include virtual prototyping, animation, surgery, robotics, cooperative design, and education among many others. Haptics is one area where the computational requirement associated with the resolution in real-time of the dynamics and contact forces of the virtual environment is particularly challenging. The paper describes various methodologies and algorithms that address the computational challenges associated with interactive simulations involving multiple contacts and impacts between human-like structures.

1 Introduction

The successful introduction of robotics into human environments will rely on the development of competent and practical systems that are dependable, safe, and easy to use. To work, cooperate, assist, and interact with humans, the new generation of robot must have mechanical structures that accommodate the interaction with the human and adequately fit in his unstructured and sizable environment. Human-compatible robotic structures must integrate mobility (legged or wheeled) and manipulation (preferably bi-manual), while providing the needed access to perception and monitoring (head camera) (Hirai et al. 1998; Takanishi et al. 1998; Khatib et al. 1999; Asfour et al. 1999; Nishiwaki et al. 2000). These requirements imply robots with branching structures - tree-like topology involving much larger numbers of degrees of freedom than those usually found in conventional industrial robots. The substantial increase in the dimensions of the corresponding configuration spaces of these robots renders the set of fundamental problems associated with their modeling, programming, planning, and control much more challenging.

The first of these challenges is the whole-robot modeling, motion coordination, and dynamic control. For robots with human-like structures, tasks are not limited to the specification of the position and orientation of a single effector. For these robots, task descriptions may involve combinations of coordinates associated with one or both arms, the head-camera, and/or the torso among others. The remaining freedom of motion is assigned to various criteria related to the robot posture and its internal and environmental constraints.

There is a large body of work devoted to the study of motion coordination in the context of kinematic redundancy. In recent years, algorithms developed for redundant manipulators have been extended to mobile manipulation robots. Typical approaches to motion coordination of redundant systems rely on the use of pseudo or generalized inverses to solve an under-constrained or degenerate system of linear equations, while optimizing some given criterion. These algorithms are essentially driven by kinematic considerations and the dynamic interaction between the end effector and the robot's self motions are ignored.

Our effort in this area has resulted in a *task-oriented* framework for whole-robot dynamic coordination and control (Khatib et al. 1996). The dynamic coordination strategy

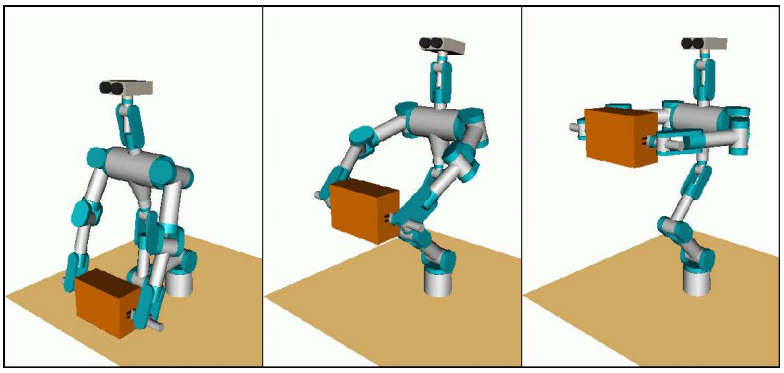

Figure 1: Manipulation and Posture Behaviors: a sequence of three snapshots from the dynamic simulation of a 24-degree-of-freedom humanoid system, whose motion is generated from simple manipulation and posture behaviors.

we developed is based on two models concerned with the task dynamics (Khatib 1987a) and the robot posture behavior. The *task dynamic behavior* model is obtained by a projection of the robot dynamics into the space associated with the task, while *the posture behavior* is characterized by the complement of this projection. To control these two behaviors, a consistent control structure is required. The paper discusses these models and presents a unique control structure that guarantees *dynamic consistency* and decoupled posture control (Khatib 1995), while providing optimal responsiveness for the task (see also Figure 1). The paper also presents recently developed recursive algorithms which efficiently address the computational challenges associated with branching mechanisms. Dynamic simulation of virtual environments is another important area of applications of these algorithms. In addition, he paper discusses our ongoing effort for the development of a general framework for interactive haptic simulation that addresses the problem of contact resolution.

A robotic system must be capable of sufficient level of competence to avoid obstacles during motion. Even when a path is provided by a human or other intelligent planner, sensor uncertainties and unexpected obstacles can make the motion impossible to complete. Our research on the artificial potential field method (Khatib 1986) has addressed this problem at the control level to provide efficient real-time collision avoidance. Due to their local nature, however, reactive methods are limited in their ability to deal with complex environments. Using navigation functions (Koditschek 1987) the problems arising from the locality of the potential field approach can be overcome. These approaches, however, do not extend well to

robots with many degrees of freedom, such as mobile manipulators. Our investigation of a framework to integrate real-time collision avoidance capabilities with a global collision-free path has resulted in the *elastic band* approach (Quinlan and Khatib 1993), which combines the benefits of global planning and reactive systems in the execution of motion tasks. The concept of elastic bands was also extended to nonholonomic robots (Khatib et al. 1997). The paper discusses our ongoing work in this area and presents extensions to the *elastic strip* approach (Brock and Khatib 2002), which enable real-time obstacle avoidance in a task-consistent manner. Task behavior can be suspended and resumed in response to changes in the environment to ensure collision avoidance under all circumstances.

Taken in conjunction, these contributions form a significant component of the the algorithmic foundation required for robots to work, assist, and cooperate with humans. Aspects of motion generation, such as task-oriented control, redundancy exploitation, or obstacle avoidance consistent with global motion objectives can be addressed by the proposed approaches, even for robots wit complex kinematic structures. In addition, the methods for simulation and haptic interaction facilitate programming of these systems in virtual environments, a much less costly and risky approach when compared to verifying the correctness of a program generating robot motion on the real robot. The ability to accurately simulate the robot's motion, in particular when in contact with the environment, is a prerequisite for the practical application of learning algorithms to fine motion generation, task execution, or similar aspects of motion.

2 Whole-Robot Control: Task and Posture

Human-like structures share many of the characteristics of macro/mini structures (Khatib 1995): coarse and slow dynamic responses of the mobility system (the macro mechanism), and the relatively fast responses and higher accuracy of the arms (the mini device). Inspired by these properties of macro/mini structures, we have developed a framework for the coordination and control of robots with human-like structures. This framework provides a unique control structure for decoupled manipulation and posture control, while achieving optimal responsiveness for the task. This control structure is based on two models concerned with the task dynamic behavior and the robot posture behavior. The *task behavior* model is ob-

tained by a projection of the robot dynamics into the space associated with the effector task, and the *posture behavior* model is characterized by the complement of this projection. We first present the basic models associated with the task. In a subsequent section we present the whole-robot coordination strategy and posture control behavior.

2.1 Task Dynamic Behavior

The joint space dynamics of a manipulator are described by

$$A(\mathbf{q})\ddot{\mathbf{q}} + \mathbf{b}(\mathbf{q}, \dot{\mathbf{q}}) + \mathbf{g}(\mathbf{q}) = \Gamma \tag{1}$$

where $\mathbf{q}$ is the n joint coordinates, $A(\mathbf{q})$ is the $n \times n$ kinetic energy matrix, $\mathbf{b}(\mathbf{q}, \dot{\mathbf{q}})$ is the vector of centrifugal and Coriolis joint forces, $\mathbf{g}(\mathbf{q})$ is the vector of gravity, and Γ is the vector of generalized joint forces.

The *operational space formulation* (Khatib 1987b) provides an effective framework for dynamic modeling and control of branching mechanisms (Russakow et al. 1995), with multiple operational points. The generalized torque/force relationship (Khatib 1987b; Khatib 1995) provides the decomposition of the total torque, Γ (equation 1) into two dynamically decoupled command torque vectors: the torque corresponding to the task behavior command vector and the torque that only affects posture behavior in the nullspace:

$$\Gamma = \Gamma_{task} + \Gamma_{posture} \tag{2}$$

For a robot with a branching structure of m effectors or operational points, the task is represented by the $6m \times 1$ vector, $\mathbf{x}$, and the $6m \times n$ Jacobian matrix is $J(\mathbf{q})$. This Jacobian matrix is formed by vertically concatenating the m $6 \times n$ Jacobian associated with the m effectors.

The task dynamic behavior is described by the operational space equations of motion (Khatib 1995)

$$\Lambda(\mathbf{x})\ddot{\mathbf{x}} + \mu(\mathbf{x}, \dot{\mathbf{x}}) + \mathbf{p}(\mathbf{x}) = \mathbf{F} \tag{3}$$

where $\mathbf{x}$, is the vector of the $6m$ operational coordinates describing the position and orientation of the m effectors, $\Lambda(\mathbf{x})$ is the $6m \times 6m$ kinetic energy matrix associated with the

operational space. $\mu(\mathbf{x}, \dot{\mathbf{x}})$, $\mathbf{p}(\mathbf{x})$, and $\mathbf{F}$ are respectively the centrifugal and Coriolis force vector, gravity force vector, and generalized force vector acting in operational space.

The joint torque corresponding to the task command vector $\mathbf{F}$, acting in the operational space is

$$\Gamma_{\text{task}} = J^T(\mathbf{q})\mathbf{F} \tag{4}$$

The task dynamic decoupling and control is achieved using the control structure

$$\mathbf{F}_{\text{task}} = \widehat{\Lambda}(\mathbf{x})\mathbf{F}^{\star}_{\text{motion}} + \widehat{\mu}(\mathbf{x}, \dot{\mathbf{x}}) + \widehat{\mathbf{p}}(\mathbf{x}) \tag{5}$$

where, $\mathbf{F}^{\star}_{\text{task}}$ represents the inputs to the decoupled system, and $\widehat{\cdot}$ represents estimates of the model parameters.

2.2 Posture Dynamic Behavior

An important consideration in the development of posture behaviors is the interactions between the posture and the task. It is critical for the task to maintain its responsiveness and to be dynamically decoupled from the posture behavior. The posture can then be treated separately from the task, allowing intuitive task and posture specifications and effective whole-robot control. The overall control structure for task and posture is

$$\Gamma = \Gamma_{\text{task}} + \Gamma_{\text{posture}} \tag{6}$$

where

$$\Gamma_{\text{posture}} = N^T(\mathbf{q})\Gamma_{\text{desired}-\text{posture}} \tag{7}$$

with

$$N(\mathbf{q}) = \left[I - \overline{J}(\mathbf{q})J(\mathbf{q})\right] \tag{8}$$

where $\overline{J}(\mathbf{q})$ is the *dynamically consistent generalized inverse* (Khatib 1995), which minimizes the robot kinetic energy

$$\overline{J}(\mathbf{q}) = A^{-1}(\mathbf{q})J^T(\mathbf{q})\Lambda(\mathbf{q}) \tag{9}$$

and

$$\Lambda(\mathbf{q}) = [J(\mathbf{q})A^{-1}(\mathbf{q})J^T(\mathbf{q})]^{-1} \tag{10}$$

This relationship provides a decomposition of joint forces into two control vectors: joint forces corresponding to forces acting at the task, $J^T\mathbf{F}$, and joint forces that only affect the robot posture, $N^T\Gamma_{\text{posture}}$. For a given task this control structure produces joint motions that minimize the robot's instantaneous kinetic energy. As a result, a task will be carried out by the combined action of the set of joints that reflect the smallest effective inertial properties.

To control the robot for a desired posture, the vector $\Gamma_{\text{desired}-\text{posture}}$ will be selected as the gradient of a potential function constructed to meet the desired posture specifications. The interference of this gradient with the task dynamics is avoided by projecting it into the dynamically consistent nullspace of $J^T(\mathbf{q})$, i.e. $N^T(\mathbf{q})\Gamma_{\text{desired}-\text{posture}}$.

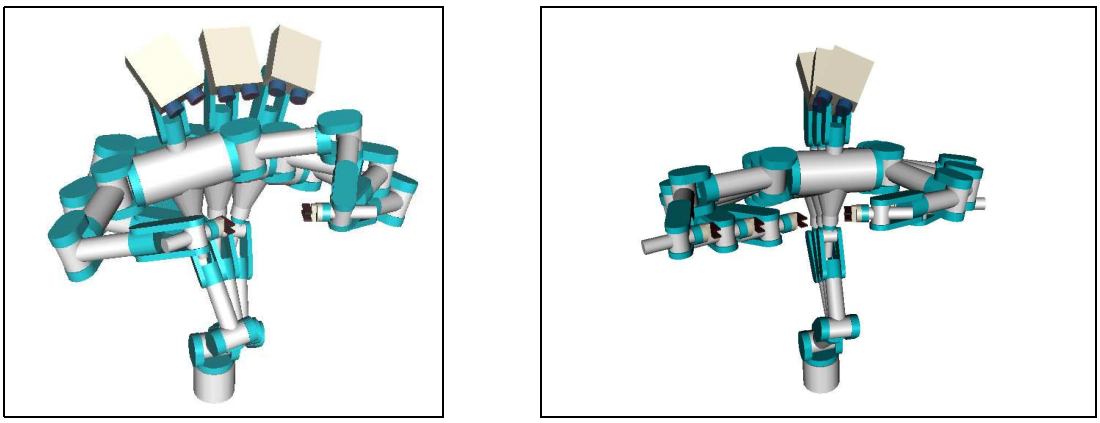

Figure 2: Dynamic Consistency and Posture Behaviors: a sequence of snapshots from the dynamic simulation of a 24-degree-of-freedom humanoid system. On the left, the task is to maintain a constant position for the two hands, while achieving hand-eye coordination. The posture motion has no effect on the task. On the right, the task also involves hand-eye coordination and motion of the common hand position. This position is interactively driven by the user. The posture is to maintain the robot total center-of-mass along the z-axis.

Dynamic consistency is the essential property for the task behavior to maintain its responsiveness and to be dynamically decoupled from the posture behavior since it guarantees not to produce any coupling acceleration in the operational space given any τ_{null}. In Figure 2 (left), the robot (a 24-degree-of-freedom humanoid system) was commanded to keep the position of both hands constant (task behavior) while moving its left and right in the

nullspace (posture behavior). Notice that dynamic consistency enables task behavior and posture behavior to be specified independently of each other, providing an intuitive control of complex systems.

For instance, the robot posture can be controlled to minimize the sum of the joint gravity torques. Such a behavior can be implemented by specifying the posture energy function to be

$$V_{\text{posture-energy}}(\mathbf{q}) = \frac{1}{2} k x_{\text{gravity}}^2 \tag{11}$$

where k is a constant gain, x_{gravity} represents the vector of the joint gravity torques. The gradient of this function

$$\Gamma_{\text{desired-posture}} = J_{\text{gravity}}^T (-\nabla V_{\text{posture-energy}}), \tag{12}$$

where J_{gravity} represents the Jacobian of the vector of gravity compensating torques, provides the required attraction to the configuration that minimized joint gravity torques. The resulting behavior is illustrated in the simulation shown in Figure 3 and Extension 1. The task shown involves three operational point associated with the arms and head.

Collision avoidance can be also integrated in the posture control as discussed in section 4. With this posture behavior, the explicit specification of the associated motions is avoided, since desired behaviors are simply encoded into specialized potential functions for various types of operations.

More complex posture behaviors can be obtained by combining various posture energies. We are currently exploring the generation of human-like natural motion from motion capture of human and the extraction of motion characteristics using human biomechanical models. For a dynamic simulation of a fully articulated human skeleton see Extension 2.

2.3 Efficient Operational Space Algorithms

Early work on efficient operational space dynamic algorithms has focused on open-chain robotic mechanisms. An efficient O(n) recursive algorithm was developed using the spatial operator algebra (Rodriguez et al. 1989; Kreutz-Delgado et al. 1991) and the articulated-body inertias (Featherstone 1987). A different approach that avoided the extra computation

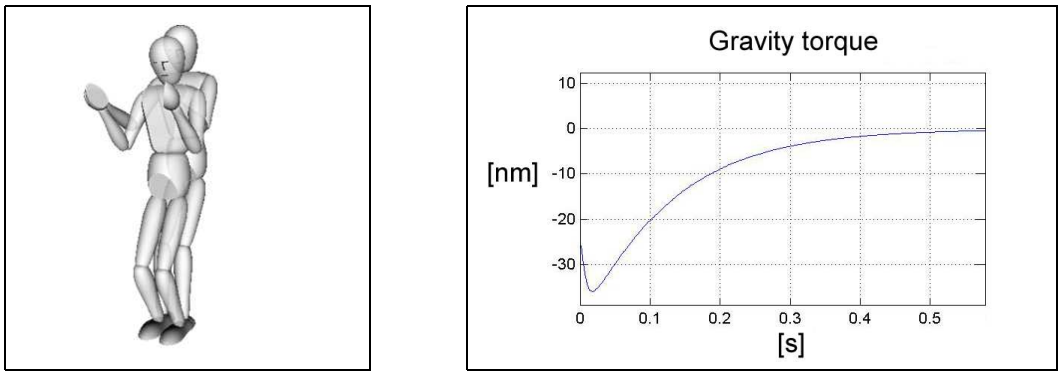

Figure 3: The robot minimizes gravity torque using postures: the task involves three operational points associated with the arms and the head while the posture motion requires the knees to minimize joint gravity torques. The starting posture has the knees of the humanoid bent. Upon activation the posture control straightens the knees to minimize gravity torques as shown in the data graph on the right.

of articulated inertias also resulted in an O(n) recursive algorithm for the operational space dynamics (Lilly 1992; Lilly and Orin 1993) Building on these early developments, our effort was aimed at algorithms for robotic mechanisms with branching structures that also address the issue of redundancy and dynamics in the nullspace.

The most computationally expensive element in the operational space whole-body control structure (equation 6) is the posture control, which involves the explicit inversion operation of the $n \times n$ joint space inertia matrix A of (equation 9), which requires $O(n^3)$. We have developed a computationally more efficient operational space control structure that eliminates the explicit computation of the joint space inertia matrix and its inverse. This elimination was achieved by combining the dynamically consistent nullspace control and the operational space control in a computationally more efficient dynamic control structure.

Using this control structure, we have developed a recursive algorithm for computing the operational space dynamics of an n-joint branching redundant articulated robotic mechanism with m operational points (Chang and Khatib 2000). The computational complexity of this algorithm is $O(nm+m^3)$, while existing symbolic methods require $O(n^3+m^3)$. Since m can be considered as a small constant in practice, this algorithm attains a linear time $O(n)$ as the number of links increases.

The algorithm proceeds by traversing the robot's branching representation both outward

(from the base to the end effectors) and inward (from the end effectors to the base); it is sketched below:

1. **Inward Recursion:** Compute the spatial operators:

$$\text{Given } {}^{h}_{i}\mathbf{X} \tag{13}$$

$${}^{h}_{i}\mathbf{L} = {}^{h}_{i}\mathbf{X}\left[\mathbf{I} - \mathbf{S}_i\overline{\mathbf{S}}_i\right] \tag{14}$$

2. **Outward Recursion:** Compute the block diagonal matrices starting with $\Omega_{0,0} = 0$:

$$\Omega_{i,i} = \mathbf{S}_i\mathbf{D}_i^{-1}\mathbf{S}_i^T + {}^{i-1}_{i}\mathbf{L}^T\Omega_{i-1,i-1}\,{}^{i-1}_{i}\mathbf{L} \tag{15}$$

3. **Outward Recursion:** Compute the block off-diagonal matrices with nearest common ancestor h of links i and j:

$$\Omega_{i,j} = \begin{cases} \text{return} & \text{if } i = j = h \\ {}^{h}_{i}\mathbf{L}^T\Omega^T_{j,h} & \text{else if } j = h \\ \Omega_{i,h}\,{}^{h}_{j}\mathbf{L} & \text{otherwise} \end{cases} \tag{16}$$

4. **Spatial Transformation:** Compute the components of the inverse operational space mass matrix with respect to the end effectors e

$$\Lambda^{-1}_{e_i,e_j} = {}^{i}_{e_1}\mathbf{X}^T\Omega_{i,j}\,{}^{j}_{e_j}\mathbf{X} \tag{17}$$

$$\Lambda^{-1}_{e} = \{\Lambda^{-1}_{e_i,e_j}\} \tag{18}$$

5. **Matrix Inversion:** Computed the extended operational space inertia matrix Λ_e, by inverting Λ^{-1}_e

where $\mathbf{S}_i$ represents the joint degrees of freedom in free space, $\overline{\mathbf{S}}_i$ represents the dynamically consistent generalized inverse of $\mathbf{S}_i$, $\mathbf{D}_i$ represents a projection of the articulated inertia (Featherstone 1987), ${}^{h}_{i}\mathbf{L}$ represents the dynamically consistent force propagator, e_i and e_j are pairs of end effectors and ${}^{h}_{i}\mathbf{X}$ represents the spatial quantity propagator (Chang and Khatib 2000). Similar algorithms are used to compute the inverse and forward dynamics, the Jacobian, the Coriolis and Centrifugal forces and the gravity forces in both joint and operational spaces (Chang 2000).

These algorithms can be used to generate dynamic simulations for complex articulated bodies. Figure 4 and Extension 3 show a simulation of a controlled jump of a skiing humanoid robot. Figure 5 shows a simulation the same robot standing up from a sitting position while manipulating a box. This simulation includes an extension of above algorithms address closed-chain branching mechanisms with a computational complexity of $O(nm+m^3)$ (Chang et al. 2000).

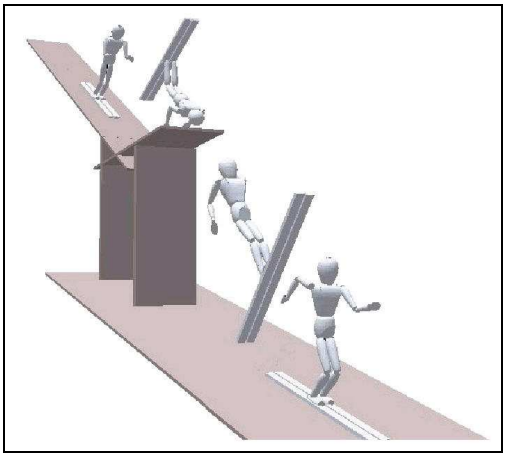

Figure 4: The image shows intermediate snapshots of a motion during a dynamic simulation involving contacts and impulses between an articulated body and its environment. The sliding motion and subsequent jump and landing are dynamically simulated in interactive time.

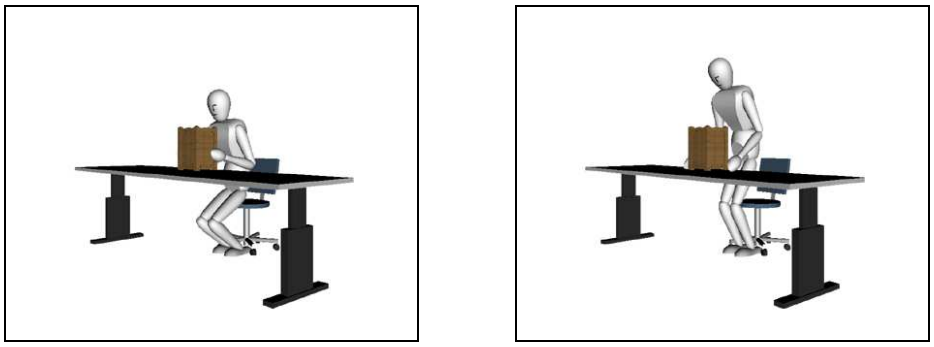

Figure 5: These two images show the motion of a humanoid robot combining task and posture constraints. Operational points at the hands are used to define the manipulation task, while another operational point on the hip permits to specify the rising behavior of the torso. Posture energies are employed to yield a natural-looking overall motion.

Other important dynamic properties and quantities of branching mechanisms can be

computed with the recursive framework presented above. One of them is the computation of reaction forces to impulses at a contact point c:

1. **Given:** $\mathbf{q}_i$, $\dot{\mathbf{q}}_i$ and $\mathbf{y}_c$

2. **Inward Recursion:** Compute the articulated-body impulse vector:

$$\mathbf{y}_{i-1}^A \quad , \quad \left(\mathbf{y}_i^A = -\,{}_c^i\mathbf{X}\mathbf{y}_c\right) \tag{19}$$

3. **Outward Recursion:** Compute the instantaneous changes in the joint velocity and the spatial velocity:

$$\Delta\mathbf{q}_i = -\mathbf{D}_i^{-1}\mathbf{S}_i^T\mathbf{y}_i^A - \overline{\mathbf{S}}_i\,{}_i^{i-1}\mathbf{X}^T\Delta\mathbf{v}_{i-1} \tag{20}$$

$$\Delta\mathbf{v}_i = {}_i^{i-1}\mathbf{X}^T\Delta\mathbf{v}_{i-1} + \mathbf{S}_i\Delta\dot{\mathbf{q}}_i \tag{21}$$

where $\mathbf{y_c}$ is the spatial impulse when the collision occurred at the contact point c.

2.4 Cooperative Manipulation

The development of effective cooperation strategies for multiple robots platforms is an important issue for both the operations in human environments and the interaction with humans. Human guided motions may involve tightly constrained cooperation performed through compliant motion actions or less restricted tasks executed through simpler free-space motion commands. Several cooperative robots, for instance, may support a load while being guided by the human to an attachment, or visually following the guide to a destination.

Our approach is based on the integration of two basic concepts: The *augmented object* (Khtaib 1988) and the *virtual linkage* (Williams and Khatib 1993). The *virtual linkage* characterizes internal forces, while the *augmented object* describes the system's closed-chain dynamics. For systems of a mobile nature, a *decentralized* control structure is needed to address the difficulty of achieving high-rate communication between platforms. In the decentralized control structure, the object level specifications of the task are transformed into individual tasks for each of the cooperative robots. Local feedback control loops are then developed

at each grasp point. The task transformation and the design of the local controllers are accomplished in consistency with the *augmented object* and *virtual linkage* models (Khtaib 1988; Williams and Khatib 1993). This approach has been successfully implemented on the Stanford robotic platforms for cooperative manipulation and human-guided motions.

3 Multi-Contact Simulation

Beyond their immediate application to physical robots, these efficient dynamic algorithms are making a significant impact on the simulation and interaction with the virtual world. The computational requirements associated with the haptic interaction with complex dynamic environments are quite challenging. In addition to the need for real-time free-motion simulation of multi-body systems, contact and impact resolution and constrained motion simulation are also needed.

Building on the operational space formulation, we developed a general framework (Ruspini and Khatib 1999) for the modeling of general multi-point collision and contact between articulated multi-body systems. The set of contact points define a task space for which an operational space inertial matrix can be constructed. This matrix Λ as in equation 10 characterizes the dynamic relationship between the contacts in the environment. In simulation the task becomes one of ensuring the the velocities and accelerations at the contact points do not permit inter-penetration. In collision, it has been shown that the configuration space velocities after collision can be modeled by the equation:

$$\dot{q}^+ = \overline{J} v^+ + \left[I - \overline{J} J \right] \dot{q}^-. \tag{22}$$

where $\overline{J}$ is the dynamically consistent inverse Jacobian for the contact space as described in equation9, and v^+ represents the desired velocities (greater then zero) at the contact points(Ruspini and Khatib 1999).

The generalized framework aids is separating the equations of motion of the system from the particular collision resolution method. Properties of the collision model can also more readily be assessed. For example for a simple empirical collision models such as $v^+ = -\epsilon v^-$, where v^+ and v^- represents the relative velocities at the contact points before and after contact it can be demonstrated that the change in kinetic energy of this model is governed

by the equation:

$$\Delta KE = (\epsilon 2 - 1)\frac{1}{2}v^{-T}\Lambda v^{-}. \tag{23}$$

As such it can be seen that the total kinetic energy of the system is conserved if the collision is completely elastic ($\epsilon = 0$) while the total energy lost during collision for an in-elastic collision ($\epsilon = 1$) is all the energy projected into the contact space.

Computing the contact space inertia matrices Λ for a number of m contact point on a branching mechanism is achieved with an efficient $O(nm + m3)$ recursive algorithm. The simulation system has been used successfully used in a teaching environment to allow students to test and debug their control algorithms before attempting to run them on a real system. Correspondence between the real and simulated system has been very close, although more rigorous systematic comparisons between the real and virtual systems is still an ongoing topic of research.

The contact space representation allows the interaction between groups of dynamic systems to be described easily without having to examine the complex equations of motion of each individual system. In addition the incorporation of haptic interaction permits a intuitive direct hands on experience.

Figure 6 and Extension 4 illustrate an example of a complex simulation involving many contacts between two humanoid figures and a number of objects. This framework was integrated with our haptic rendering system (Ruspini et al. 1997) to provide a general environment for interactive haptic dynamic simulation. The multi-contact interactions between robot and objects in the environment appear visually correct; we are currently investigating the physical fidelity of our multi-contact simulation.

4 Task-Consistent Elastic Plans

The control methods presented in Section 2 allow the consistent control of task and posture for robots with complex mechanical structures, such as human-like robots. To perform or assist in the execution of complex actions, however, these control structures have to be linked with motion generated by a planner. Furthermore, since unstructured environments can be highly dynamic, such an integration has to accommodate unforeseen obstacle motion in real

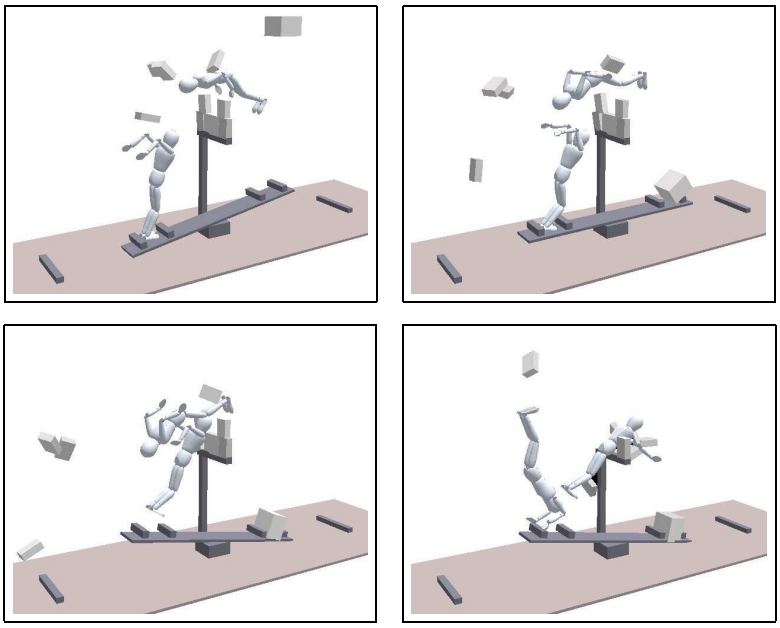

Figure 6: The sequence shows the dynamic interaction between two figures and a number of objects. The dynamics, contacts, and control are computed in interactive time.

time, while conforming to constraints imposed by the task. We have developed algorithms that perform task-consistent, real-time path modification to address this issue.

4.1 Real-Time Path Modification

The elastic band (Quinlan and Khatib 1993) was developed to allow real-time modification of a previously planned path, effectively avoiding a costly planning operation in reaction to changes in the environment. More recently, this framework was complemented by the elastic strip framework (Brock and Khatib 2002).

The elastic strip framework augments the representation of a path computed by a planner with a description of free space around that path. Collision avoidance can be guaranteed, if the work space volume swept by the robot along its path is contained within the free space. Real-time path modification is implemented by subjecting the entire path to an artificial potential field (Khatib 1986), keeping the path at a safe distance from obstacles. The modification of the path in accordance with those potentials is performed while ensuring that the volume swept by the robot along the path is always contained within the representation of local free space. This results in "elastic" paths, which deform in reaction to approaching

obstacles, while maintaining the global properties of the path.

In addition to the repulsive, external potential, we also apply internal forces to consecutive configurations of the robot along the path. This shortens and smoothes the path. The overall behavior of of a path represented in the elastic strip framework can be compared to a string of elastic material: as obstacles approach, the path is locally modified or "stretched" by repulsive forces; once the obstacle moves further away, internal forces shorten and smooth the path. Such behavior is shown in the top left image of Figure 7. The end effector of the robot is commanded to move on a straight line. The original path generated by the planner is a simple straight-line motion, as no obstacles are present. The image shows the path after two mobile obstacles move into the path.

The elastic strip framework scales to robots with many degrees of freedom and with many operational points, as it avoids a costly search for collision-free motion in configuration space. Instead, it employs simple work space-based potential fields in conjunction with aforementioned control structures to modify a previously planned motion in real time.

4.2 Task-Consistent Path Modification

In dynamic environments it is desirable to integrate reactive obstacle avoidance with task behavior. To accomplish this we extend the overall control structure for task and posture behavior (equation 2) by adding torques $\Gamma_{obstacle}$ representing desired obstacle avoidance behavior:

$$\Gamma = \Gamma_{task} + \Gamma_{posture} + \Gamma_{obstacle}$$

Both, $\Gamma_{posture}$ and $\Gamma_{obstacle}$ have been mapped into the nullspace of the task, as shown in equation 7. Using this control structure, the task-consistent obstacle avoidance behavior shown in the second image of Figure 7 is achieved. Note how without task-consistency the end effector deviates significantly from the required straight-line trajectory. Using task-consistent obstacle avoidance, the end effector only deviates minimally from the task, as can be seen in the graphs shown in Figure 7 (see also Extensions 5, 6, and 7).

This approach of integrating task and obstacle avoidance behavior can fail, however, when the torques resulting from mapping Γ_{obstacle} into the nullspace yield insufficient motion

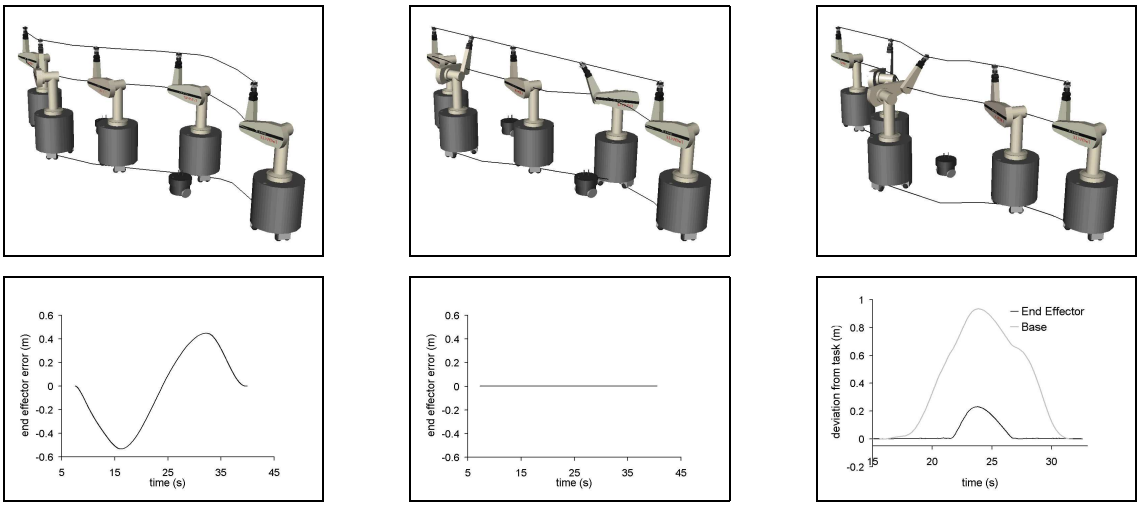

Figure 7: Top images show from left to right: real-time obstacle avoidance without task consistency, with task consistency, and transitioning between task-consistent and non task-consistent behavior. Lines indicate trajectories of the base, elbow, and end effector. The end-effector task is to follow a straight-line trajectory. Without task-consistency the end-effector deviates significantly from the task, as shown in the leftmost image and graph. With task consistency, the end-effector is following a straight line and the end-effector error is minimal (middle image and graph). On the right, the task of following a straight-line trajectory is suspended; the corresponding graph shows the trajectory of the base and the associated end-effector error.

to ensure obstacle avoidance. In such a situation it would be desirable to suspend task execution and to realize obstacle avoidance with all degrees of freedom of the robot.

Using the dynamically consistent nullspace, $\mathcal{N}(J(\mathbf{q}))$ of equation 8, associated with the task. The coefficient

$$c = \frac{\|N^T(J(\mathbf{q}))\ \Gamma_{\text{obstacle}}\|}{\|\Gamma_{\text{obstacle}}\|}$$

corresponds to the ratio of the magnitude of the torque vector Γ_{obstacle} mapped into that nullspace to its unmapped magnitude. This coefficient is an indication of how well the behavior represented by Γ_{obstacle} can be performed inside the nullspace of the task. We experimentally determine a value c_s at which it is desirable to suspend task execution in favor of the behavior previously mapped into the nullspace. Once the coefficient c assumes a value $c < c_s$, a transition is initiated. During this transition task behavior is gradually suspended and previous nullspace behavior is performed using all degrees of freedom of the

manipulator. The motion of the manipulator is now generated using the equation

$$\Gamma = \alpha \left[J^T(\mathbf{q})\, \mathbf{F} + \mathcal{N}^T(J(\mathbf{q}))\, \Gamma_{\text{obstacle}} \right] + \overline{\alpha}\, \Gamma_{\text{obstacle}} \tag{24}$$

where $\alpha \in [0..1]$ is a time-based transition variable, transitioning between 1 and 0 during task suspension and between 0 and 1 during resumption of the task, and $\overline{\alpha} = (1 - \alpha)$ is defined as the complement of α.

The experimental results, performed on the Stanford Assistant Manipulator, for such transitioning behavior can be seen in Figure 7. The image on the top right shows how despite task-consistent obstacle avoidance the task has to be suspended to ensure obstacle avoidance. Below, the graph shows how the base deviates significantly from the straight line in response to the obstacle. The end effector, however, maintains the task until it has to be suspended. The graph also shows that the task is resumed in a smooth manner, after the base has passed the obstacle.

Task-consistent modification with the elastic strip framework was also demonstrated in experiments on the Stanford Robotic Platform (see Figure 8 and Extension 8). During these experiments the end-effector error generally did not exceed $2mm$; in some experiments motion with sub-millimeter error was achieved. The motion of the obstacle, a Scout robot, is perceived using a SICK laser range finder.

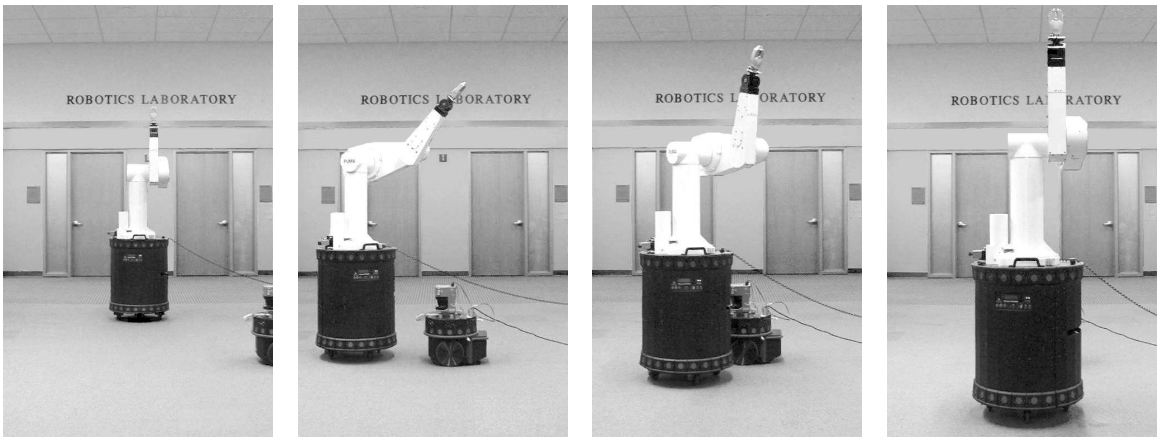

Figure 8: Demonstrating task-consistent obstacle avoidance with the Stanford Robotic Platform. The end-effector performs a straight-line motion, while the base avoids the obstacle, which is perceived using a laser range finder.

5 Conclusion

Advances toward the challenge of robotics in human environments depend on the development of the basic capabilities needed for both autonomous operations and human/robot interaction. In this article, we have presented methodologies for whole-robot coordination and control, cooperation between multiple robots, interactive haptic simulation with contact, and the real-time modification of collision-free path to accommodate changes in the environment.

For the whole-robot coordination and control, we presented a framework which provides the user with two basic task-oriented control primitives: task control and posture control. The major characteristic of this control structure is the dynamic consistency it provides in implementing these two primitives: the robot posture behavior has no impact on the end-effector dynamic behavior. While ensuring dynamic decoupling and improved performance, this control structure provides the user with a higher level of abstraction in dealing with task specifications and control.

Addressing the computational challenges of human-like robotic structures, we presented efficient $O(nm+m^3)$ recursive algorithms for the operational space dynamics of mechanisms involving branching structures and closed chains. Building on the operational space formulation, we also developed a framework for the resolution of multi-contact between articulated multi-body systems. The computational efficiency of the dynamic algorithms developed for physical robots provided the interactivity needed for haptic simulation of complex virtual environments.

The elastic strip framework allows the integration of obstacle avoidance with the task-oriented control structure. It provides for real-time motion generation that combines obstacle avoidance and task execution. When kinematic or external constraints imposed by obstacles make it impossible to maintain the task, task-consistent obstacle avoidance is suspended and all degrees As the constraints are relaxed, the task is resumed in a smooth manner. Using the elastic strip framework, motion for complex kinematic structures can be generated very efficiently, as the required computations are mostly performed in work space and as a result are independent of the number of degrees of freedom of the mechanism.

Acknowledgments

The financial support of Honda and NSF (grants IRI-9320017) is gratefully acknowledged. Many thanks to Alan Bowling, Arancha Casal, Francois Conti, Robert Holmberg, Jaeheung Park, Costas Stratelos, James Warren, and Kazuhito Yokoi for their valuable contributions to the work reported here.

References

Asfour, T., K. Berns, J. Schelling, and R. D. nn (1999). Programming of minipulation tasks of the humanoid rob ot armar. In *Proceedings of the International Conference on Advanced Robotics*.

Brock, O. and O. Khatib (2002). Elastic strips: A framework for motion generation in human environments. *International Journal of Robotics Research 21*(12), 1031–1052.

Chang, K.-S. (2000). *Efficient Dynamic Control and Simulation of Highly Redundant Articulated Mechanisms*. Ph. D. thesis, Stanford University.

Chang, K.-S., R. Holmberg, and O. Khatib (2000, April). The augmented object model: Cooperative manipulation and parallel mechanism dynamics. In *Proceedings of the International Conference on Robotics and Automation*, San Francisco, CA, U.S.A., pp. 470–47.

Chang, K.-S. and O. Khatib (2000, April). Operational space dynamics: Efficient algorithms for modeling and control of branching mechanisms. In *Proceedings of the International Conference on Robotics and Automation*, San Francisco, CA, U.S.A., pp. 850–856.

Featherstone, R. (1987). *Robot Dynamics Algorithms*. Kluwer Academic Publishers.

Hirai, K., M. Hirose, Y. Haikawa, and T. Takenaka (1998). The development of honda humanoid robot. In *Proceedings of the International Conference on Robotics and Automation*, Volume 2, Leuven, Belgium, pp. 1321–1326.

Khatib, M., H. Jaouni, R. Chatila, and J.-P. Laumond (1997). How to implement dynamic paths. In *Proceedings of the International Symposium on Experimental Robotics*, pp.

225–36. Preprints.

Khatib, O. (1986). Real-time obstacle avoidance for manipulators and mobile robots. *International Journal of Robotics Research 5*(1), 90–8.

Khatib, O. (1987a). A unified approach to motion and force control of robot manipulators: The operational space formulation. *International Journal of Robotics Research 3*(1), 43–53.

Khatib, O. (1987b, February). A unified approach to motion and force control of robot manipulators: The operational space formulation. *International Journal of Robotics and Automation RA–3*(1), 43–53.

Khatib, O. (1995). Inertial properties in robotics manipulation: An object-level framework. *International Journal of Robotics Research 14*(1), 19–36.

Khatib, O., K. Yokoi, O. Brock, K.-S. Chang, and A. Casal (1999). Robots in human environments: Basic autonomous capabilities. *International Journal of Robotics Research 18*(7), 175–183.

Khatib, O., K. Yokoi, K.-S. Chang, D. Ruspini, R. Holmberg, and A. Casal (1996). Coordination and decentralized cooperation of multiple mobile manipulators. *Journal of Robotic Systems 13*(11), 755–64.

Khtaib, O. (1988). Object manipulation in a multi-effector robot system. In R. Bolles and B. Roth (Eds.), *Robotics Research 4*, pp. 137–144. MIT Press.

Koditschek, D. E. (1987). Exact robot navigation by means of potential functions: Some topological considerations. In *Proceedings of the International Conference on Robotics and Automation*, pp. 1–6.

Kreutz-Delgado, K., A. Jain, and G. Rodriguez (1991, April). Recursive formulation of operational space control. In *Proceedings of the International Conference on Robotics and Automation*, pp. 1750–1753.

Lilly, K. W. (1992). *Efficient Dynamic Simulation of Robotic Mechanisms*. Kluwer Academic Publishers.

Lilly, K. W. and D. E. Orin (1993, September/October). Efficient O(n) recursive computation of the operational space inertia matrix. *IEEE Transactions on Systems, Man,*

and Cybernetics 23(5), 1384–1391.

Nishiwaki, K., T. Sugihara, S. Kagami, F. Kanehiro, M. Inaba, and H. Inoue (2000). Design and development of research platform for perception-action integration in humanoid robot : H6. In *Proceedings of the International Conference on Intelligent Robots and Systems*, Volume 3, pp. 1559–1564.

Quinlan, S. and O. Khatib (1993). Elastic bands: Connecting path planning and control. In *Proceedings of the International Conference on Robotics and Automation*, Volume 2, pp. 802–7.

Rodriguez, G., K. Kreutz, and A. Jain (1989, May). A spatial operator algebra for manipulator modeling and control. In *Proceedings of the International Conference on Robotics and Automation*, pp. 1374–1379.

Ruspini, D. C. and O. Khatib (1999, October). Collision/contact models for dynamic simulation and haptic in teraction. In *9th International Symposium of Robotics Research (ISRR'99)*, Snowbird, Utah, U.S.A., pp. 185–195.

Ruspini, D. C., K. Kolarov, and O. Khatib (1997, August). The haptic display of complex graphical environments. In *SIGGRAPH Conference Proceedings (Computer Graphics)*, Los Angeles, CA, U.S.A., pp. 345–352. ACM SIGGRAPH.

Russakow, J., O. Khatib, and S. M. Rock (1995). Extended operational space formation for serial-to-parallel chain (branching) manipulators. In *Proceedings of the International Conference on Robotics and Automation*, Volume 1, pp. 1056–1061.

Takanishi, A., S. Hirano, and K. Sato (1998). Development of an anthropomorphic head-eye system foå humanoid robot-realization of human-like head-eye motion using eyelids adjusting to brightness. In *Proceedings of the International Conference on Robotics and Automation*, Volume 2, Leuven, Belgium, pp. 1308–1314.

Williams, D. and O. Khatib (1993). The virtual linkage: A model for internal forces in multi-grasp manipulation. In *Proceedings of the International Conference on Robotics and Automation*, Volume 1, pp. 1025–30.

List of Figures

List of Multi-Media Extensions

Extension 1

Type: Video

File: extension01.mpg

Caption: Task and posture control sequence. The task involves the control of the position of the hands and the orientation of the head. The posture is designed to minimize the gravity torques at the knee joint. As the desired position of the two hands is changed interactively, the robot moves them into the desired position while optimizing the posture constraint.

Extension 2

Type: Video

File: extension02.mpg

Caption: The motion of a human skeleton is generated by dynamic simulation. The user interactively excerts a force onto the skeleton at a location indicated by the mouse pointer at times 0:04 and 0:07. The dynamic response of the skeleton is shown in the video.

Extension 3

Type: Video

File: extension03.mpg

Caption: A humanoid figure on skis is dropped on a ski jump. The only actuation is provided by gravitational forces. All subsequent interactions with the environment are determined using the described framework for dynamic multi-contact simulation.

Extension 4

Type: Video

File: extension04.mpg

Caption: A dynamically simulated sequence involving two humanoids and many objects in the environment.

Extension 5

Type: Video

File: extension05.mpg

Caption: Real-time path modification using elastic strips. To avoid the obstacles, the mobile manipulator deviates significantly from the task, which consists of following the red line with the end-effector.

Extension 6

Type: Video

File: extension06.mpg

Caption: Task-consistent path modification using elastic strips. The obstacles perform the same motion as in the previous video. Obstacle avoidance is performed in the nullspace of the task so that task execution is not interrupted.

Extension 7

Type: Video

File: extension07.mpg

Caption: Obstacle motion renders task-consistent path modification impossible, due to kinematic limitations of the mechanism. Based on the elastic strip framework, the task is automatically suspended and resumed when the second obstacle is avoided.

Extension 8

Type: Video

File: extension08.mpg

Caption: The experiments shown in Extensions 7 and 8 are executed on a real robot.